LETTER

Effect of Cs on the Stability and Photovoltaic Performance of 2D/3D Perovskite-Based Solar Cells

Lior Iagher and Lioz Etgar*

The Institute of Chemistry, The Center for Nanoscience and Nanotechnology, The Casali Center for Applied Chemistry, The Hebrew University of Jerusalem, Jerusalem 9190401, Israel

S *Supporting Information*

ABSTRACT: One of the attractive features of hybrid perovskite is the possibility to reduce its dimensionality, which enhances the perovskite's resistivity to moisture. In this work, we used 2D/3D perovskites to study different organic molecular spacers (aromatic ring vs cyclic ring); Cs was introduced as an additional small cation to methylammonium. It was found that Cs improves the photovoltaic performance; however, it reduces the cells' stability because two cations having a different ionic radius are mixed, which creates strains in the perovskite structure. The aromatic ring spacers display better stability in complete cells than does the cyclo spacer. Importantly, Cs has a greater effect on the stability than does the nature of the spacer molecule. The difference in the size of the organic cations as well as the inorganic cations plays a major role in the perovskite's stability in a film and in a complete solar cell.
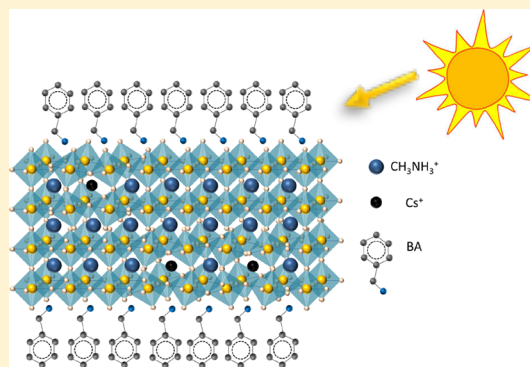
Three-dimensional (3D) perovskite-based solar cells achieved PCEs of around 22%;[1] however, the moisture and long-term use remain a concern for large-scale device manufacturing. Perovskite structures with the general chemical formula of AMX_3 represent a class of materials with a cubic unit cell. Here A is a monovalent cation that could be organic, as in the case of methylammonium (MA), and inorganic, such as cesium; M is a divalent metallic compound, usually Pb^{2+}, and X is a monovalent halide anion such as $I^−$, $Br^−$, or $Cl^−$.

In recent years, low-dimensional perovskite has been embedded in several solar cell structures including planar TiO_2 and mesoporous TiO_2.[2,3] Low-dimensional perovskite solar cells exhibit better resistance to degradation processes because of moisture over their three-dimensional counterparts. The two-dimensional perovskite is fabricated by utilizing a large organic cation with a large ionic radius that does not fit into the 3D perovskite structure and thus creates a layered perovskite structure where the large cations act as a spacer in the inorganic lead halide octahedral framework. The inorganic framework is composed of a corner-sharing octahedron $[MX_6]^{4−}$ that is derived from the parent 3D perovskite. The organic cations are attracted by ionic and hydrogen bonds to the inorganic framework, and as a result, the inorganic layers are confined and stacked together.[4,5] In such a layered structure, a quantum well is formed, and the dielectric constant of the organic barrier molecules is lower than the dielectric constant of the inorganic

lead halide octahedral framework. Thus, the spacer molecule acts as the barrier and the inorganic framework acts as the well. The dielectric and quantum confinement in the case of low *n* values will result in higher band gap energies.[6−8]

Tsai et al.[9] used *n*-butylammonium (BUA) as a spacer in a perovskite structure of the formula $(BUA)_2(MA)_3Pb_4I_{13}$ ($n = 4$). The low-dimensional perovskite functioned as the light harvester in a planar architecture, achieving a high PCE of 12.51%. Improved performance, compared with earlier studies, was achieved by using the hot-casting one-step deposition technique, which forms well-oriented perovskite layers in which the inorganic framework is vertical with respect to the substrate, allowing pathways for better charge transport through the perovskite film toward the contacts. The two-dimensional (2D) perovskite solar cells (PSCs) exhibited enhanced stability over their 3D counterparts. Zhang et al.[10] fabricated the same cell structure using the same spacer but with the addition of 5% Cs, achieving 13.68% efficiency.

Grancini et al.[11] utilized ammonium valeric acid iodide (AVAI) as a cation spacer and fabricated a combination of 2D/3D $(AVAI)_2PbI_4/MAPbI_3$ perovskites using fully printable industrial scale processes to fabricate a solar module with a carbon-based architecture. The solar module achieved a power

conversation efficiency (PCE) of 11.2% and exhibited stable PV performance under 1 sun illumination for 1 year. Recently utilized 2D/3D perovskites, based on a mixed cation, formamidinium (FA) with Cs, and mixed halides (iodide and bromide) using the BUA cation as a spacer, were used in a solar cell.[12] The stability of these cells was measured under constant illumination, and they were exposed to 40−50% humidity; the results show slightly enhanced stability for the 2D/3D-based cells compared with the 3D-based cells.

Motivated by previous studies that showed better stability for the 2D, 2D/3D, and quasi-2D perovskites over the 3D perovskite while maintaining high PV performance,[12−14] we studied their effect on the stability and PV performance when using 2D/3D perovskite with different barrier molecules (aromatic vs cyclic) and mixed cations, i.e., Cs and methylammonium (MA). MA is known to be one of the driving forces for decomposing the perovskite because of its sublimation and its reaction with oxygen, which can create a free oxygen radical, which in turn can react with the perovskite and/or with the hole transporting material (HTM), thus accelerating the decomposition process.[15−17]

The 2D/3D perovskite synthesized in this study is related to the formula $(R-NH_3)_2(A)_{n-1}Pb_nI_{3n+1}$, where A represents $CH_3NH_3^+$ (MA) or, in the mixed cation configuration, the ratio between MA^+ and Cs^+ (i.e., $MA_{1-x}Cs_x$) and $R-NH_3$ represent the barrier molecules, which were used in this study, as shown in Figure 1: phenethylammonium iodide, $C_8H_{12}NI$ (PEA); cyclohexylammonium iodide, $C_6H_{14}NI$ (CHMA); and benzylammonium iodide, $C_7H_{10}NI$ (BA). The 2D and 2D/3D perovskites were synthesized by the addition of
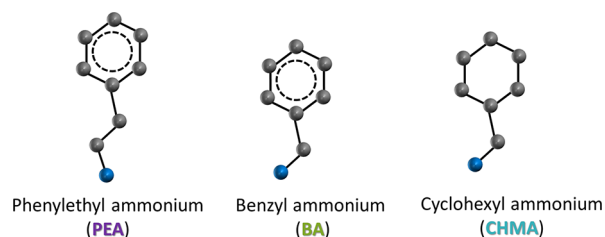
MAI, PbI_2, a barrier molecule, and Cs in appropriate stoichiometric quantities in order to achieve the desired n value. Detailed description of the sample and solar cell preparation is presented in the Supporting Information (SI).

Figure 2A presents X-ray diffraction (XRD) measurements of the synthesized 2D perovskite films ($n = 1$) using different barriers. The XRD results confirm the formation of pure 2D perovskite by the absence of peaks that are ascribed to 3D tetragonal perovskite at angles of 14.2°, which correspond to a crystallographic plane (110), and at angles of 28.5°, which correspond to a crystallographic plane (220). The dominate reflections are related to the (00l) planes, suggesting the preferential c-axis growth of the crystals.[18] The presence of higher-order peaks suggests that the films are highly oriented and have excellent crystallinity. The d spacings of the different perovskites are 16.3, 16.8, and 14.4 Å for PEA, CHMA, and BA, respectively. The difference in the d spacing between the benzene derivative molecules, namely, PEA and BA, is related to the additional methylene group that may influence the orientation and length between adjacent inorganic lead halide octahedral frameworks. However, the difference in d spacing between BA and CHMA is due to the aromatic ring (in BA) and the nonaromatic ring (in CHMA), which influence the C−C bond length.

To elucidate the optical properties of 2D perovskite ($n = 1$), absorbance was measured, as shown in Figure 2B. The absorbance spectra are slightly shifted between the barriers, where BA is red-shifted compared with CHMA and PEA; these results are in good agreement with previous reports.[19] As discussed previously, the band gap energy of low n values increased owing to quantum and dielectric confinement. By introducing different organic cations, the Pb−I−Pb angle deviated, owing to various orientations and hydrogen bonding, which cause in- and out-of-plane distortions of the inorganic framework. As a result, the band gap energies are slightly shifted between the barrier molecules.[20]

In addition to 2D perovskite, where $n = 1$, 2D/3D perovskite (where $n = 40$) was synthesized in order to incorporate it into photovoltaic cells. The absorbance of the 2D/3D perovskite films displays band gap energies similar to those of the 3D perovskite (Figure 3A,B). At low n values, the band gap energy increases; however, at higher n values, there is no confinement due to the increasing thickness of the inorganic framework. Furthermore, the absorbance spectra do not exhibit excitonic

Figure 1. Schematic structure of the different barriers (R-NH₃): phenethylammonium iodide (PEA), benzylammonium iodide (BA), and cyclohexylammonium iodide (CHMA).
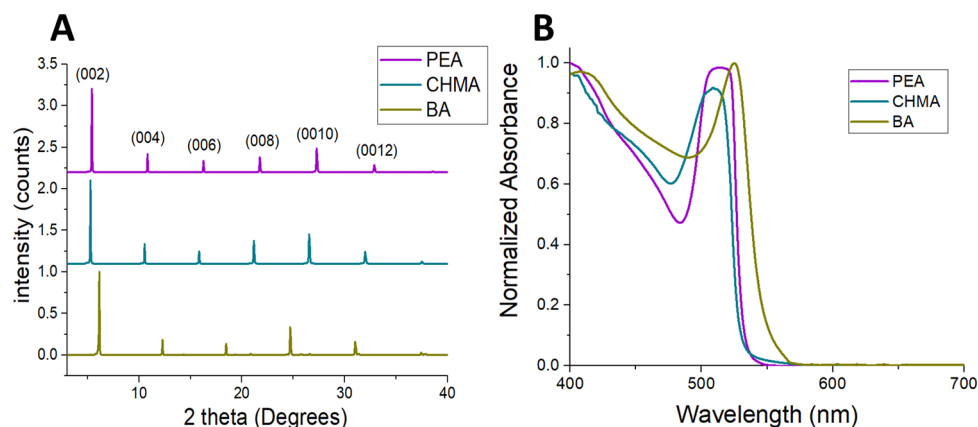
Figure 2. (A) XRD patterns of the 2D layered perovskite structure $n = 1$ of the different barrier molecules. (B) Absorbance spectra of the corresponding barrier molecules.
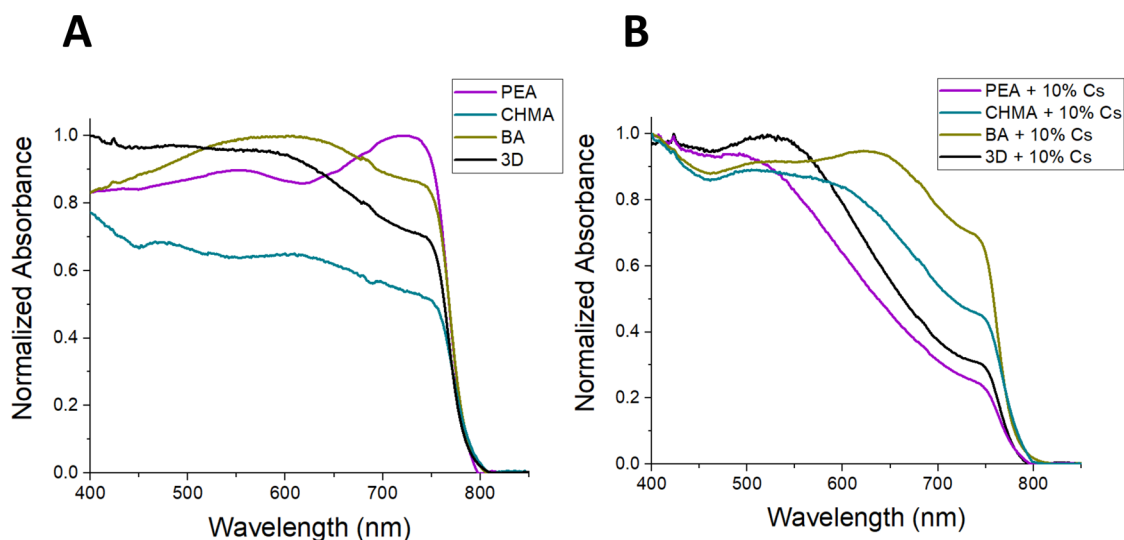
Figure 3. (A) Absorbance spectra of the 2D/3D ($n = 40$) perovskite structure of the different barrier molecules and of the 3D perovskite. (B) Absorbance spectra of 2D/3D ($n = 40$) perovskite with the addition of 10% Cs, using the different barrier molecules, and of the 3D mixed with the addition of 10% Cs.
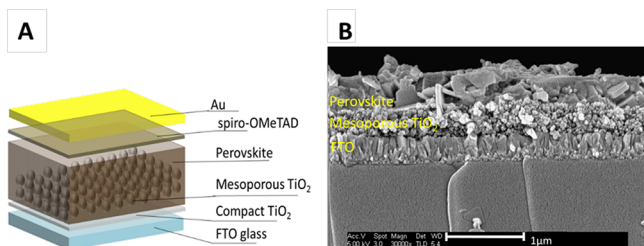
Figure 4. (A) Solar cell used in this study. (B) HR-SEM cross section of the solar cell with the 2D/3D ($n = 40$) perovskite, where the CHMA is the barrier molecule.

behavior, suggesting the presence of free carriers, which is opposite to the case of low n values, where the exciton binding energy is higher than kT, which results in transport properties similar to those of the 2D/3D perovskite and the 3D perovskite.

Photovoltaic Performance. Following the physical and optical characterization, we incorporated the 2D/3D ($n = 40$) perovskite with the different barrier molecules into the solar cell structure presented in Figure 4A. A high-resolution scanning electron microscopy (HR-SEM) cross section of the studied solar cells is shown in Figure 4B. The solar cell consists of FTO glass, compact and mesoporous TiO_2 layers with thicknesses of 50 and 350 nm, respectively, followed by perovskite as the light harvester, with a thickness of ca. 400 nm,

and HTM (spiro-OMeTAD) on top of the perovskite. Finally, gold contacts were evaporated with a thickness of 70 nm.

Previous work carried out in our lab showed that at low n values the perovskite transport properties are not good enough to deliver high PV performance,[21] whereas in the case of high n values, i.e., 2D/3D perovskite, the PV performance can be enhanced compared with the 3D perovskite. Therefore, in this work, a 2D/3D perovskite structure, corresponding to high n values, was used in the solar cell. All solar cells were fabricated with stoichiometry corresponding to $n = 40$, i.e., 2D/3D perovskite.

The PV performance of the PSCs is summarized in Tables 1 and 2, and the current−voltage ($J–V$) curves of the best-performing cells are presented in Figure 5A,B. The 2D/3D PSCs without Cs and with Cs (i.e., mixed cations, Cs, and MA) have a PV performance similar to their 3D counterparts. The Cs concentration used in these cells is 10%, which gives the best PV performance; other PV results for different Cs concentrations can be found in Table 1S in the Supporting Information. The addition of Cs to the perovskite structure enhances the PV performance significantly, both with open-circuit voltage (V_{oc}) and short-circuit current (J_{sc}), resulting in higher PCEs of these cells compared with the case without Cs.

The best PV performance for the 2D/3D system was observed with 10% Cs and PEA as the barrier molecule. The cell achieved 14.33% efficiency with a V_{oc} value of 0.92 V, a J_{sc} value of 25.5 mA/cm^2, and a fill factor of 61%. The external

Table 1. Average Photovoltaic Results and the Best Photovoltaic Results (in Brackets) of the Different Barrier Molecules and the 3D Perovskite

barrier molecule	V_{oc} (V)	J_{sc} (mA/cm^2)	fill factor (%)	efficiency (%)	hysteresis loss (%)
PEA	0.86 ± 0.04	20.8 ± 1.8	56 ± 3	9.9 ± 0.6	12.15
	(0.85)	(23.1)	(56.3)	(11.06)	
BA	0.85 ± 0.04	20.6 ± 1.8	57 ± 5	10.0 ± 1.0	11.01
	(0.90)	(22.7)	(57.8)	(11.89)	
CHMA	0.86 ± 0.06	20.4 ± 3.5	59 ± 4	10.2 ± 0.9	5.24
	(0.86)	(21.6)	(61.8)	(11.54)	
3D perovskite	0.90 ± 0.06	20.0 ± 2.0	60 ± 7	10.7 ± 1.2	14.3
	(0.94)	(22.1)	(56.8)	(11.86)	

Table 2. Average Photovoltaic Results and the Best Photovoltaic Results (in Brackets) of the Different Barrier Molecules and 3D Perovskite Using 10% Cs

barrier molecule	V_{oc} (V)	J_{sc} (mA/cm^2)	fill factor (%)	efficiency (%)	hysteresis loss (%)
PEA + 10% Cs	0.90 ± 0.02 (0.92)	24.0 ± 1.0 (25.5)	59 ± 2 (61.0)	12.6 ± 0.9 (14.33)	24.49
BA + 10% Cs	0.86 ± 0.04 (0.93)	21.4 ± 1.8 (22.4)	55 ± 3 (52.5)	10.2 ± 0.6 (11.00)	22.72
CHMA + 10% Cs	0.86 ± 0.01 (0.90)	21.9 ± 1.5 (23.6)	56 ± 2 (58.9)	10.6 ± 1.3 (12.58)	11.9
3D + 10% Cs	0.87 ± 0.08 (0.99)	23.9 ± 0.7 (24.9)	54 ± 4 (59.0)	11.3 ± 1.9 (14.61)	21.33
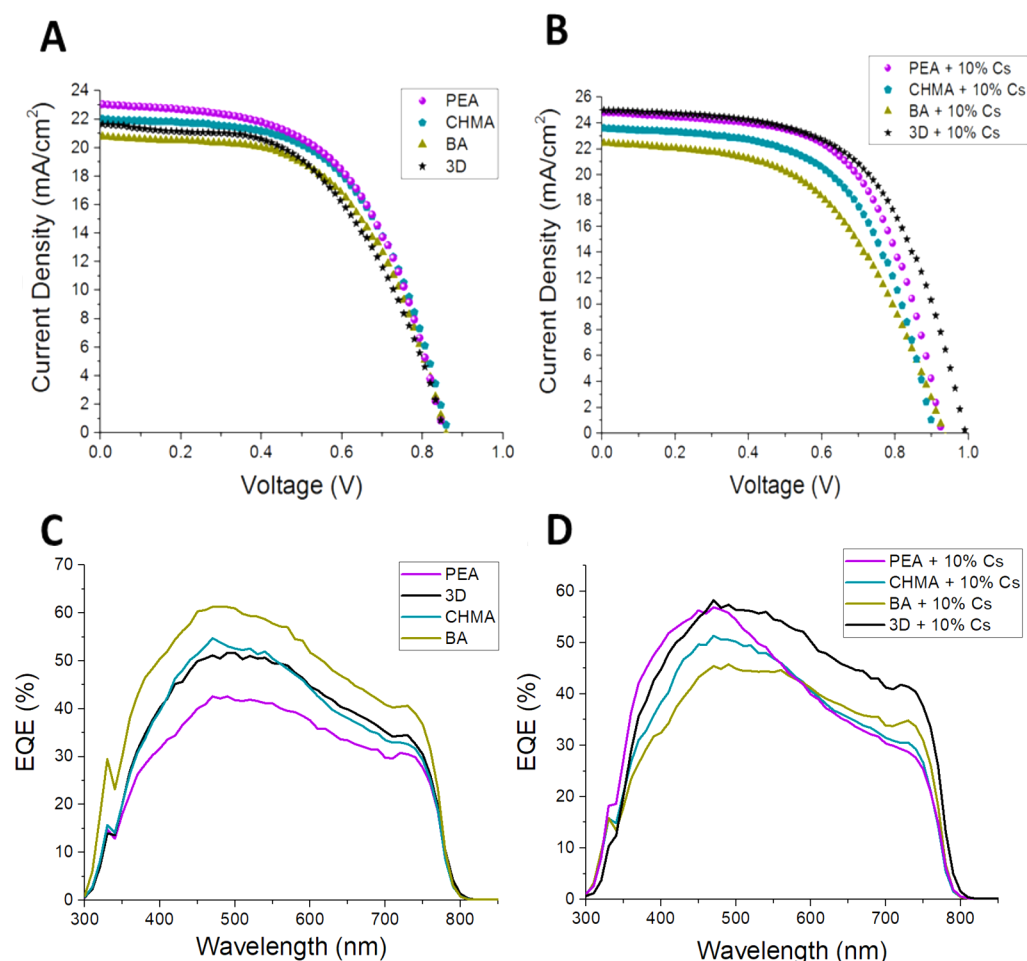
Figure 5. (A) Current density−voltage (J−V) curves of the best-preforming solar cells based on the 2D/3D perovskite (n = 40) using the different barriers and the 3D perovskite. (B) Current density−voltage (J−V) curves of the best-preforming solar cells based on the 2D/3D mixed cation perovskite (n = 40) using the different barriers and of 3D mixed cation perovskite. (C) EQE of the best-preforming solar cells based on the 2D/3D perovskite (n = 40) using the different barriers and the 3D perovskite. (D) EQE of the best-preforming solar cells based on the 2D/3D mixed cation perovskite (n = 40) using the different barriers and the 3D mixed cation perovskite.

quantum efficiency (EQE) spectra are presented in Figure 5C,D; the EQE shape is in good agreement with the absorbance spectra, and the trend of the integrated J_{sc} matches the trends measured under AM1.5G standard irradiation. The differences between the integrated J_{sc} (results shown in Tables 2S and 3S) and the J_{sc} value, measured by the solar simulator, are due to the reason that during the solar simulator measurements the cells operate at a maximum power point, whereas in the case of the EQE measurements, the cells operate at a point lower than the maximum power point.

In order to quantify the hysteresis of these cells, we developed eq 1, which takes the area below the J−V curves and subtracts the forward curve scan from the reverse curve scan. The hysteresis loss calculated using eq 1 is shown in Table 1.

In general, the hysteresis loss from those cells based on a mixed cation (with Cs) is higher compared with the MA-based cells (without Cs). The proposed mechanism for the hysteresis in PSCs is mainly due to trap-assisted recombination at the grain boundaries, which is amplified by ion migration toward the grain boundaries.[22] As discussed, the perovskite structure of mixed cation (MA and Cs) could be more distorted than that
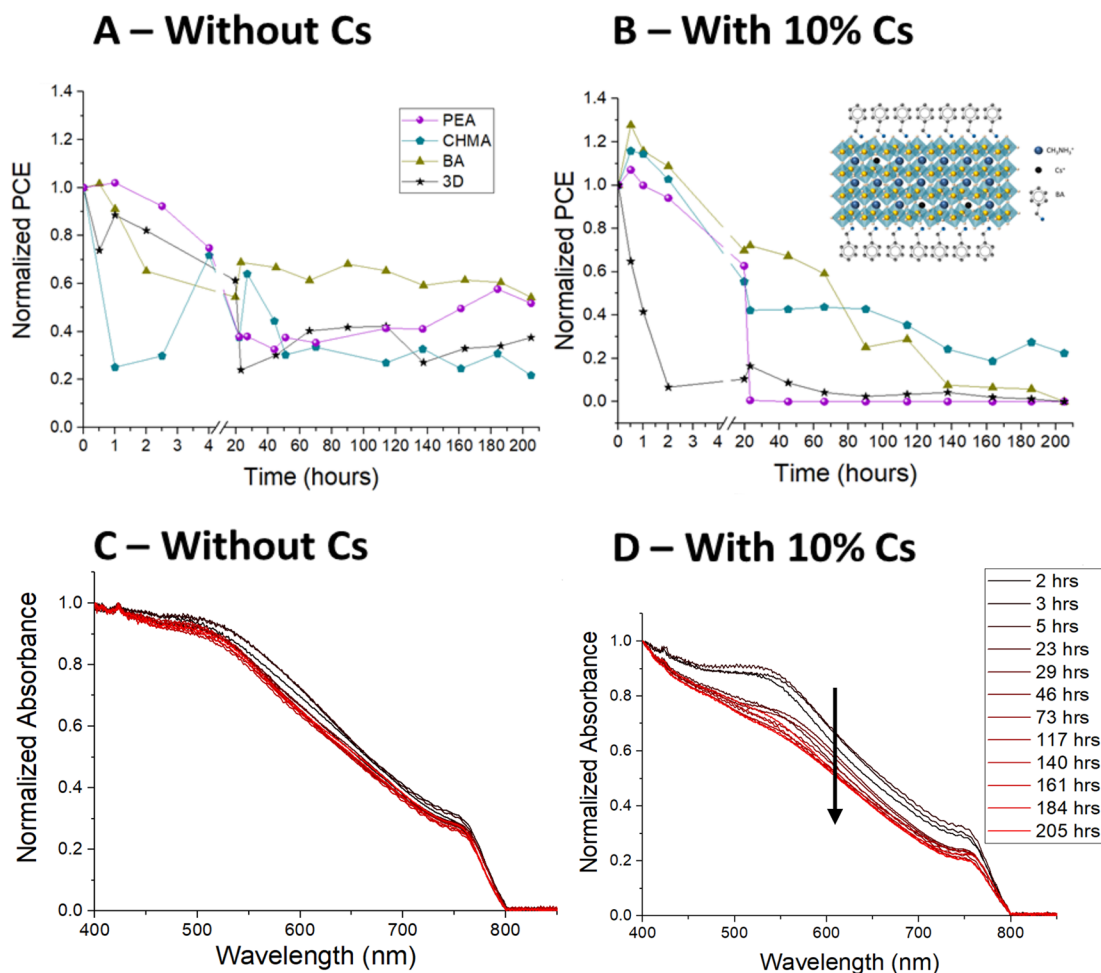
Figure 6. (A) Stability measurements of solar cells based on 2D/3D perovskites (n = 40) of the different barriers and of the 3D perovskite under 1 sun illumination, 30−50% humidity, and for 205 h. (B) Stability measurements of solar cells based on 2D/3D mixed cation perovskites (n = 40) of the different barriers and of the 3D mixed cation perovskite under 1 sun illumination, 30−50% humidity, and for 205 h. (Inset) Schematic illustration of distorted layered mixed cation MA + Cs perovskite with CHMA as a spacer. (C) Absorbance stability over the time of 2D/3D (n = 40) perovskites films based on BA as a spacer. (D) Absorbance stability over time of the 2D/3D (n = 40) mixed cation MA + Cs perovskite films based on BA as a spacer.

without incorporating Cs; therefore, films based on these perovskite structures could potentially have higher defect densities and, therefore, more pronounced hysteresis. Furthermore, because the barrier molecule is shorter, the hysteresis loss is smaller, e.g., BA and CHMA barriers. The reason for that could be due to charge accumulation, which is influenced by the barrier molecule. As the barrier molecule becomes longer, the charge accumulation in the perovskite layer becomes higher, which results in more pronounced hysteresis.[19,21]

$$P = \sum_{j=0}^{J_{sc}} (j \cdot dv)$$

$$\text{Hysteresis Loss} = P_{\text{forward}} - P_{\text{reverse}} \left(\frac{\text{mW}}{\text{cm}^2} \right)$$

$$\text{Hysteresis Loss \%} = \frac{\text{Hysteresis Loss}}{P_{\text{forward}}} \cdot 100 \qquad (1)$$

Stability. The PV performance of the different solar cells stored in the dark under N$_2$ environment over a period of 40 days is presented in Figure 1SA,1SB in the Supporting Information. The PCE of the cells (with and without Cs) did

not display a drop in performance of more than 10% compared with their initial values; on the contrary, some cells showed improved PV performance over this period. The improvement in the performance could be related to crystallization processes, which occur over time and because of the evaporation of trapped solvent in the cells.

In order to investigate the stability of the fabricated PSCs, we carried out stability measurements of encapsulated PSCs under AM1.5G illumination, with temperatures of 50−60 °C in the chamber and a humidity of 40−50%. The results are shown in Figure 6A,B. Several observations can be concluded from these measurements: (i) The mixed cation MA + Cs-based cells display relatively poor stability compared with their MA-based cells. A possible reason for that is related to the mixing of two cations with different ionic radiuses, which creates strains in the perovskite structure (see the inset of Figure 6B for a schematic illustration); similar observations have been described in previous studies.[23,24] The increase in strains and distortions, in turn, could accelerate the degradation process. (ii) The CHMA-based cells exhibit better stability with the mixed cation cells. This could be explained by the nature of the aliphatic ring, which helps facilitate the polar NH$_3^+$ functional group and thus
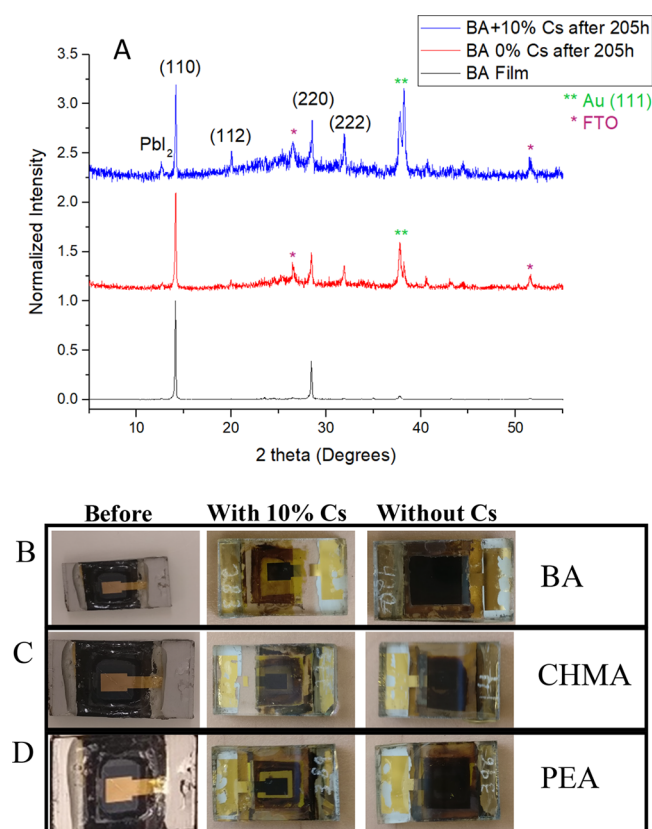
Figure 7. (A) XRD diffractograms of BA-based 2D/3D ($n = 40$) perovskites: black, fresh film of BA as a spacer; red, perovskite solar cell based on BA as a spacer after 205 h of constant illumination with 50% humidity. (B) Photo of the solar cell before the stability measurements. (C) Photo of the solar cell based on a mixed cation (Cs + MA) and the corresponding spacer after the stability measurements. (D) Photo of the solar cell based on the corresponding spacer after the stability measurements.

minimizes the distortion of the inorganic framework caused by adding the Cs.

With the MA-based cells (i.e., without Cs), the stability of the PSCs seems to be improved when the barrier molecule has an aromatic ring. The observed enhanced stability for the BA and PEA cells could be due to the increased hydrophobicity and stronger VDW interactions in these layered perovskite structures of the spacer cations with aromatic benzene derivatives, compared with the aliphatic CHMA cation spacer and compared with 3D cells, which do not have any spacer cation. Importantly, apparently the effect of Cs on the stability is stronger than the aromatic vs aliphatic effect, as observed from these results.

Furthermore, we measured the absorbance for the two 2D/3D perovskites with and without Cs using the same barrier molecule, i.e., BA, under the same stability conditions as the complete cells. The absorbance results support the results obtained for the complete cells (see Figure 6C,D). The BA films without Cs did not show any sign of degradation because the absorbance onset does not change and the intensity of the absorbance above 500 nm wavelength shows a minimal decrease over time. With the mixed cation films (with Cs), some degradation is observed over time because the intensity of the absorbance of wavelengths above 500 nm decreases. On the basis of the absorbance stability measurements, which do not include a HTM layer, it can be concluded that a major factor

causing the degradation is related to the HTM (i.e., spiro-OMeTAD), which was also discussed in previous studies.[25,26]

In order to further characterize the stability of the fabricated PSCs, we investigated the crystallinity of 2D/3D perovskites based on BA. The XRD from a fresh film of BA was compared with films (of 2D/3D with and without Cs) after 205 h of 1 sun illumination and 50% humidity. The XRD spectra (Figure 7A) of the 2D/3D mixed cation (Cs + MA) show traces of PbI_2 as opposed to the freshly made film and to the 2D/3D film without Cs that has not shown any traces of PbI_2. These XRD results further support the findings that the single small cation-based cells exhibited better stability compared with the mixed cation-based cells. Figure 7B−D shows photos of solar cells with the studied spacers before and after the stability measurements. It can be concluded that in the case of the mixed cation the cells changed to yellow after the stability measurements, which is not the case with the cells of a single small cation.

In this work, we studied how different barrier molecules and incorporating Cs affect the 2D/3D perovskite structure. It was found that the PV performance improved when Cs was added as a second small cation to the 2D/3D perovskite. On the other hand, the stability of the complete solar cells decreased with the addition of the Cs. The spacer molecules did not appreciably affect the PV performance of the cells; however, the stability of the solar cells was affected because of the spacer molecules. The aromatic spacer molecules show better stability than does the cyclo spacer molecule. The increase in the number of strains and distortions in the perovskite structure due to the difference in the size of the small cations, Cs^+ vs MA^+, could accelerate the degradation process of the perovskite

■ ASSOCIATED CONTENT

S Supporting Information

The Supporting Information is available free of charge on the ACS Publications website at DOI: 10.1021/acsenergylett.7b01196.

> Description of the experimental details, stability under dark, and PV results of the different Cs concentrations (PDF)

■ AUTHOR INFORMATION

Corresponding Author

*E-mail: lioz.etgar@mail.huji.ac.il.

ORCID

Lioz Etgar: 0000-0001-6158-8520

Notes

The authors declare no competing financial interest.

■ REFERENCES

(1) Yang, W. S.; Park, B. W.; Jung, E. H.; Jeon, N. J.; Kim, Y. C.; Lee, D. U.; Shin, S. S.; Seo, J.; Kim, E. K.; Noh, J. H.; et al. Iodide management in formamidinium-lead-halide−based perovskite layers for efficient solar cells. *Science* **2017**, *356*, 1376−1379.

(2) Stoumpos, C. C.; Soe, C. M.; Tsai, H.; Nie, W.; Blancon, J. C.; Cao, D. H.; Liu, F.; Traore, B.; Katan, C.; Even, J.; et al. High members of the 2D Ruddlesden-Popper halide perovskites: synthesis,

optical properties, and solar cells of $(CH_3(CH_2)_3NH_3)_2(CH_3NH_3)_4Pb_5I_{16}$. *Chem.* **2017**, *2*, 427−440.

(3) Safdari, M.; Svensson, P. H.; Hoang, M. T.; Oh, I.; Kloo, L.; Gardner, J. M. Layered 2D alkyldiammonium lead iodide perovskites: synthesis, characterization, and use in solar cells. *J. Mater. Chem. A* **2016**, *4*, 15638−15646.

(4) Mitzi, D. B. Templating and structural engineering in organic−inorganic perovskites. *J. Chem. Soc., Dalton Trans.* **2001**, *0*, 1−12.

(5) Mitzi, D. B.; Feild, C.; Harrison, W.; Guloy, A. Conducting tin halides with a layered organic-based perovskite structure. *Nature* **1994**, *369*, 467−469.

(6) Muljarov, E. A.; Tikhodeev, S. G.; Gippius, N. A.; Ishihara, T. Excitons in self-organized semiconductor/insulator superlattices: PbI-based perovskite compounds. *Phys. Rev. B: Condens. Matter Mater. Phys.* **1995**, *51*, 14370−14378.

(7) Ishihara, T. Optical properties of PbI-based perovskite structures. *J. Lumin.* **1994**, *60−61*, 269−274.

(8) Ishihara, T.; et al. Dielectric confinement effect for exciton and biexciton states in PbI-based two-dimensional semiconductor structures. *Surf. Sci.* **1992**, *267*, 323−326.

(9) Tsai, H.; Nie, W.; Blancon, J. C.; Stoumpos, C. C.; Asadpour, R.; Harutyunyan, B.; Neukirch, A. J.; Verduzco, R.; Crochet, J. J.; Tretiak, S.; et al. High-efficiency two-dimensional Ruddlesden − Popper perovskite solar cells. *Nature* **2016**, *536*, 312−317.

(10) Zhang, X.; Ren, X.; Liu, B.; Munir, R.; Zhu, X.; Yang, D.; Li, J.; Liu, Y.; Smilgies, D. M.; Li, R.; et al. Stable high efficiency two-dimensional perovskite solar cells via cesium doping. *Energy Environ. Sci.* **2017**, *10*, 2095−2102.

(11) Grancini, G.; Roldan-Carmona, C.; Zimmermann, I.; Mosconi, E.; Lee, X.; Martineau, D.; Narbey, S.; Oswald, F.; De Angelis, F.; Grätzel, M.; et al. One-year stable perovskite solar cells by 2D/3D interface engineering. *Nat. Commun.* **2017**, *8*, 15684−15692.

(12) Wang, Z.; Lin, Q.; Chmiel, F. P.; Sakai, N.; Herz, L. M.; Snaith, H. J. Efficient ambient-air-stable solar cells with 2D−3D hetero-structured-butylammonium-caesium-formamidinium lead halide perovskites. *Nat. Energy* **2017**, *2*, 17135−17145.

(13) Quan, L. N.; Yuan, M.; Comin, R.; Voznyy, O.; Beauregard, E. M.; Hoogland, S.; Buin, A.; Kirmani, A. R.; Zhao, K.i; Amassian, A.; et al. Ligand-stabilized reduced-dimensionality perovskites. *J. Am. Chem. Soc.* **2016**, *138*, 2649−2655.

(14) Smith, I. C.; Hoke, E. T.; Solis-Ibarra, D.; McGehee, M. D.; Karunadasa, H. I. A layered hybrid perovskite solar-cell absorber with enhanced moisture stability. *Angew. Chem., Int. Ed.* **2014**, *53*, 11232−11235.

(15) Berhe, T. A.; Su, W. N.; Chen, C. H.; Pan, C. J.; Cheng, J. H.; Chen, H. M.; Tsai, M. C.; Chen, L. Y.; Dubale, A. A.; Hwang, B. J. Organometal halide perovskite solar cells: degradation and stability. *Energy Environ. Sci.* **2016**, *9*, 323−356.

(16) Habisreutinger, S. N.; Leijtens, T.; Eperon, G. E.; Stranks, S. D.; Nicholas, R. J.; Snaith, H. J. Carbon nanotube/polymer composites as a highly stable hole collection layer in perovskite solar cells. *Nano Lett.* **2014**, *14*, 5561−5568.

(17) Ono, L. K.; Schulz, P.; Endres, J. J.; Nikiforov, G. O.; Kato, Y.; Kahn, A.; Qi, Y. Pinhole-free hole transport layers significantly improve the stability of MAPbI$_3$-based perovskite solar cells under operating conditions. *J. Phys. Chem. Lett.* **2014**, *5*, 1374−1379.

(18) Mitzi, D. B.; Prikas, M. T.; Chondroudis, K. Thin film deposition of organic-inorganic hybrid materials using a single source thermal ablation technique. *Chem. Mater.* **1999**, *11*, 542−544.

(19) Cohen, B. E.; Wierzbowska, M.; Etgar, L. High efficiency quasi 2D lead bromide perovskite solar cells using various barrier molecules. *Adv. Funct. Mater.* **2017**, *1*, 1935−1943.

(20) Knutson, J. L.; Martin, J. D.; Mitzi, D. B. Tuning the band gap in hybrid tin iodide perovskite semiconductors using structural templating. *Inorg. Chem.* **2005**, *44*, 4699−4705.

(21) Cohen, B. E.; Wierzbowska, M.; Etgar, L. High efficiency and high open circuit voltage in quasi 2D perovskite based solar cells. *Adv. Funct. Mater.* **2017**, *27* (5), 1604733−1604740.

(22) Snaith, H. J.; Abate, A.; Ball, J. M.; Eperon, G. E.; Leijtens, T.; Noel, N. K.; Stranks, S. D.; Wang, J. T. W.; Wojciechowski, K.; Zhang, W. Anomalous hysteresis in perovskite solar cells. *J. Phys. Chem. Lett.* **2014**, *5*, 1511−1515.

(23) Mitzi, D. B.; Dimitrakopoulos, C. D.; Kosbar, L. L. Structurally tailored organic-inorganic perovskites: Optical properties and solution-processed channel materials for thin-film transistors. *Chem. Mater.* **2001**, *13*, 3728−3740.

(24) Xu, Z.; Mitzi, D. B.; Dimitrakopoulos, C. D.; Maxcy, K. R. Semiconducting perovskites $(2\text{-}XC_6H_4C_2H_4NH_3)_2SnI_4$ (X = F, Cl, Br): Steric interaction between the organic and inorganic layers. *Inorg. Chem.* **2003**, *42*, 2031−2039.

(25) Yang, J.; Siempelkamp, B. D.; Liu, D.; Kelly, T. L. Investigation of $CH_3NH_3PbI_3$ degradation rates and mechanisms in controlled humidity environments using in situ techniques. *ACS Nano* **2015**, *9* (2), 1955−1963.

(26) Sanehira, E. M.; Tremolet de Villers, B. J.; Schulz, P.; Reese, M. O.; Ferrere, S.; Zhu, K.; Lin, L. Y.; Berry, J. J.; Luther, J. M. Influence of electrode interfaces on the stability of perovskite solar cells: reduced degradation using MoO$_x$/Al for hole collection. *ACS Energy Lett.* **2016**, *1*, 38−45.